



Impact of rotational errors of whole pelvis on the dose of prostate-based image-guided radiotherapy to pelvic lymph nodes and small bowel in high-risk prostate cancer

Hiroki Katayama¹, Shigeo Takahashi², Takuya Kobata¹, Akihiro Oishi¹, Toru Shibata²

¹Department of Clinical Radiology, Kagawa University Hospital, Kagawa, Japan

²Department of Radiation Oncology, Kagawa University Hospital, Kagawa, Japan

ABSTRACT

Background: The target volume increases when the prostate and pelvic lymph nodes (PLNs) are combined, and the fiducial markers (FMs) are placed at the edge of the irradiation field. Thus, the position of FMs may be changed by the rotational errors (REs) of “whole pelvis”. The aim of this study was to examine the impact of REs of “whole pelvis” on the dose of FMs-based image-guided radiotherapy to the PLNs and the small bowel in prostate cancer including the PLNs.

Materials and methods: We retrospectively evaluated 10 patients who underwent prostate cancer radiotherapy involving the PLNs. The position of FMs was calculated from the radiographs obtained before and after the 6D correction of pelvic REs. We simulated the delivery dose considering the daily pelvic REs and calculated the difference from the planned dose in the $D_{98\%}$ of the PLN clinical target volume and the D_{2cc} and V_{45Gy} of the small bowel.

Result: The position of FMs strongly correlated with the pelvic REs in the pitch direction ($r = 0.7788$). However, the mean delivered doses to PLNs for 10 patients were not significantly different from the planned doses ($p = 0.625$). Although the D_{2cc} and V_{45Gy} of the small bowel strongly correlated with the pitch rotation of the pelvis, there was no significant difference between the delivered and planned doses ($p = 0.922$ and $p = 0.232$, respectively).

Conclusion: The dosimetric effect of pelvic REs on the dose to PLNs and the small bowel was negligible during the treatment course.

Key words: rotational errors; image-guided radiotherapy (IGRT); pelvic lymph nodes; prostate cancer; fiducial marker

Rep Pract Oncol Radiother 2021;26(6):906-914

Introduction

High-risk prostate cancer is treated with a combination of radiotherapy and hormone therapy, and the pelvic lymph nodes (PLNs) may be included in the clinical target volume (CTV) [1]. The prostate and PLNs can be treated with the simultaneous integrated boost (SIB) technique [2].

Online image-guided radiotherapy (IGRT) based on the fiducial markers (FMs) in prostate can reduce rectal doses and toxicities [3, 4]. The effect of prostate-based IGRT on the dose to PLNs and organs at risk (OAR) was investigated in cases where both the prostate and PLNs were treated simultaneously [5-8]. Eminowicz et al. [5] simulated the dose to PLNs by applying the incremental 1-mm

Address for correspondence: Hiroki Katayama, Ph.D., Department of Clinical Radiology, Kagawa University Hospital, Kagawa, Japan 1750-1 Ikenobe, Miki-cho, Kita-gun, Kagawa 761-0793, Japan, tel: (+81)87-898-5111, fax: (+81)87-891-2351; e-mail: k-hiroki@med.kagawa-u.ac.jp

This article is available in open access under Creative Common Attribution-Non-Commercial-No Derivatives 4.0 International (CC BY-NC-ND 4.0) license, allowing to download articles and share them with others as long as they credit the authors and the publisher, but without permission to change them in any way or use them commercially

isocenter (IC) shifts in the treatment planning system in each direction, and reported that the risk of inadequate PLNs coverage was less than 1%. Nunen et al. [2] reported the differences in OAR dose for the bone match and prostate match.

The target volume increases when the prostate and PLNs are combined, and the entire pelvis need to be irradiated. For treatment planning, the FMs are placed at the edge of the irradiation field because the IC position will be placed at the center of the target volume. For patient setup, rotational errors (REs) of “whole pelvis” lead to displacement at the ends of the target volume [9]. Thus, the magnitude of IC shifts will be changed by the displacement of the position of FMs because of pelvic REs, which might be the cause of increased risk to the small bowel or decreased dose to the PLNs.

In previous studies, the pelvic REs were never corrected before the prostate-based IGRT and only the 3D cone beam computed tomography (CBCT)-based [6,8] or 3D FM-based matching [10] was performed.

First, we investigated the impact of pelvic REs on the position of FMs using the radiographs obtained before and after correction of the pelvic REs. Second, we evaluated the effect of the correction of pelvic REs on the dose to PLNs and small bowels by simulating the daily IC shifts and pelvic REs.

Materials and methods

Patient selection

This study was approved by our institutional ethics board. We retrospectively evaluated 10 patients who underwent volumetric modulated arc therapy (VMAT) for prostate cancer, including the PLNs, between March 2015 and November 2017. Nine patients had two FMs (VISICOIL™; IBA Dosimetry, Bartlett, TN, USA), and one patient had one FM implanted in the prostate. The patients were immobilized in a supine position using a Hip-Fix, Vac-Lok cushion (CIVCO, Kalona, IA, USA) and heel support, and were instructed to fill their bladder 1 hour prior to planning computed tomography (CT) acquisition. The planning CT images were acquired using an Aquilion LB (Canon Medical Systems Corp., Tokyo, Japan) with a slice thickness of 2 mm.

Treatment planning

The contours, which had been delineated by a single radiation oncologist, were as follows: the

prostate, seminal vesicles, bladder, rectum, femoral heads, small bowel, large bowel, and PLNs. The prostate CTV includes the whole prostate and seminal vesicles and was expanded by 9 mm in all directions, except the posterior direction in which a 5-mm expansion was used to form the planning target volume (PTV) of the prostate. The delineation of the CTV for the PLNs (CTV_{LN}) was based on consensus recommendations from the RTOG contouring guidelines [11]. The CTV_{LN} was expanded by 5 mm in all directions to form the PTV for the PLNs (PTV_{LN}). The small and large bowels were contoured by individual loops. When the overlap of contours between the small bowel and PTV_{LN} occurred, the small bowel was prioritized to achieve constraints.

For each patient, the VMAT plan with three arcs was constructed in Eclipse ver.11.0.31 (Varian Medical Systems, Palo Alto, CA, USA). All treatment plans were created with simultaneous integrated boost technique in 39 fractions using 10 MV photons. The IC position was placed at the center of the entire treatment volume, including both targets (prostate PTV + PTV_{LN}) [2, 12]. An example of the IC and the position of FMs for treatment planning is shown in Supplementary File — Figure S1. The dose was prescribed 78 Gy to the prostate PTV, and 58.5 Gy to the PTV_{LN}. The dose objectives of the small bowel were as follows: $V_{30\text{Gy}} < 50\%$ and $V_{45\text{Gy}} < 10\%$. Dose calculation was performed using the AcurosXB algorithm. All patients were treated with a Clinac iX linear accelerator (Varian Medical Systems, Palo Alto, CA, USA).

IGRT strategy

All treatments were performed by using the routine ExacTrac X-ray IGRT system. (BrainLAB AG, Germany). The IGRT protocol of our institution consists of two steps. In the first step, after setup using a laser, two oblique radiographs are obtained, and then a 6 D bone matching is performed by comparing with the digitally reconstructed radiographs (DRRs) generated from the planning CT. In the second step, two oblique radiographs are obtained, and the 3D FMs matching is performed. 3D calculation of the position of FMs with the ExacTrac system is performed by manual matching of the FMs between the radiographs and DRRs. Thus, the radiographs were obtained before and after correction of the pelvic REs (defined as radiographs A and B in this study, respectively).

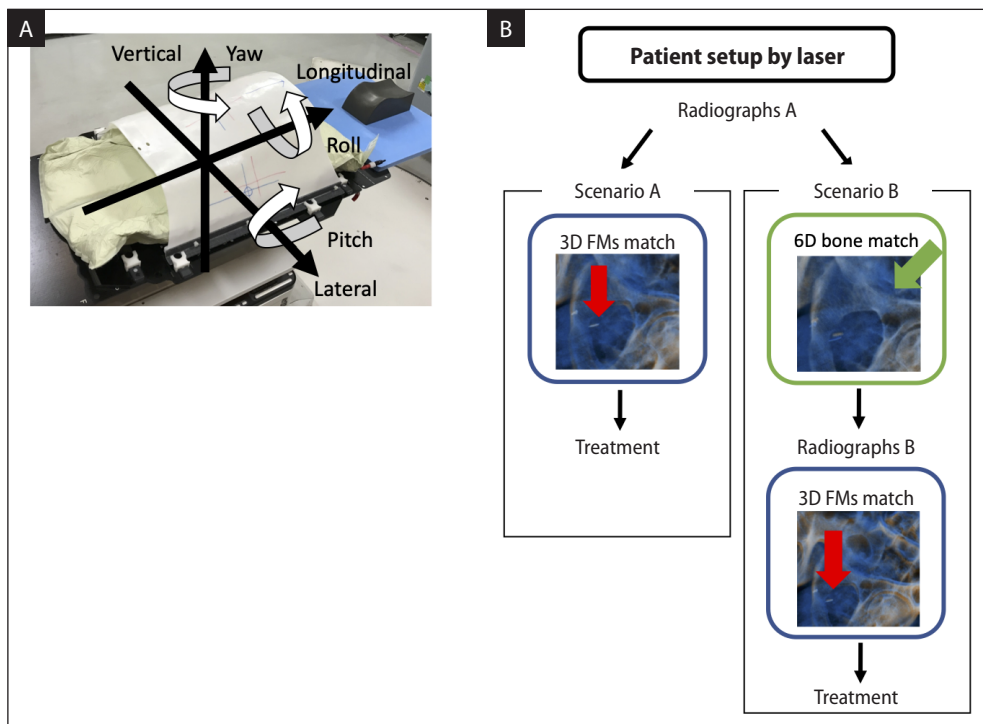


Figure 1.A. Patient position and the coordinate system; arrows indicate positive translation and rotation with respect to each axis in this study; **B.** Flowchart of image-guided radiotherapy (IGRT) simulations from patient setup to treatment. Scenario A was simulated on the basis of the 3D FM matches, performed under conditions of uncorrected pelvic REs, using radiographs A, and scenario B was simulated on the basis of the 3D FM matches after 6D bone matches using radiographs B. The red and green arrows indicate the FMs and bone matches between the digitally reconstructed radiographs (DRRs) and radiographs

Pelvic REs and 3D positions of FM

Figure 1A shows the definition of positive translation and rotation with respect to each axis in this study. We obtained the pelvic REs from radiographs A for all treatments. Next, we calculated the 3D displacement of FMs from their position on the planning CT images and compared them between radiographs A and B. Moreover, we examined the correlations between directions of pelvic REs and the difference in FM positions before and after the correction of pelvic REs.

Simulations

Figure 1B shows the flowchart of IGRT scenario simulation. Scenario A was simulated based on 3D FMs matching using radiographs A, i.e., the 3D FM matching was performed under conditions of uncorrected pelvic REs. Scenario B was simulated based on 3D FM matching using radiographs B.

Simulation of scenario A

Pelvic REs during the course of treatment were simulated based on the rotations of planning CT

images. Planning CT images with the contours were transferred to the MIM maestro Ver. 6.4 (MIM Software Inc., Cleveland, OH, USA). We created the rotated CT images using the “Edit rotation” tool of the MIM, which can rotate all CT images in all directions and to any magnitude and can generate new CT images. The rotated CT images were created based on the pelvic REs obtained from radiographs A, which were generated for all fractions. These CT images with the contours were transferred to the Eclipse for dose calculation. The IC position was determined based on the corresponding point on the original plan on the rotated CT images and shifted on the basis of the FM position calculated from radiographs A. Dose calculation was performed using the same monitor unit (MU) and multi-leaf collimator (MLC) motion as that in the original plan for all fractions.

Simulation of scenario B

We assumed that pelvic REs was completely removed by the 6D bone match, and we did not con-

sider residual rotational errors. The IC position in the original plan on the planning CT images was shifted based on the FM position obtained from radiographs B, and re-calculation of the dose distribution was performed by using the same MU and MLC motion as that in the original plan for all fractions.

Difference in DVH parameters from planned dose for each scenario

We examined the differences in dose volume histogram (DVH) parameters from planned dose in each scenario and compared them between scenario A and B.

For each fraction dose, the differences in $D_{98\%}$ of CTV_{LN} (Gy) and D_{2cc} of the small bowel (Gy) from the planned dose were calculated as follows:

$$Dose\ difference\ (\%) = \frac{D_{scenario} - D_{plan}}{D_{plan}} \times 100 \quad (1)$$

where $D_{scenario}$ and D_{plan} are the doses for each scenario and the original plan, respectively.

The difference in V_{45Gy} of the small bowel (%) from the plan volume was calculated as follow:

$$Volume\ difference\ (\%) = V_{scenario} - V_{plan} \quad (2)$$

where $V_{scenario}$ and V_{plan} are the volumes for each scenario and the original plan, respectively.

Next, we calculated the differences in DVH parameters between scenarios A and B as follows:

$$D_{diff}\ (\%) = \frac{D_{scenarioA} - D_{scenarioB}}{D_{plan}} \times 100 \quad (3)$$

$$V_{diff}\ (\%) = V_{scenarioA} - V_{scenarioB} \quad (4)$$

where D_{diff} indicates the difference in $D_{98\%}$ of CTV_{LN} (Gy) or D_{2cc} of the small bowel (Gy) and V_{diff} indicates the difference in V_{45Gy} of the small bowel (%). We examined the correlations between the directions of the pelvic REs and the differences in DVH parameters between scenarios A and B.

Estimation of the delivery dose during a treatment course for each scenario

For individual patients, the cumulative delivered dose for the entire course of therapy was calculated based on the sum of the fraction doses in each sce-

nario. We compared the original planned dose and cumulative delivered dose in scenarios A and B for ten patients.

Statistical analysis

Statistical analysis was performed using JMP® 13 (SAS Institute Inc., Cary, NC, USA). Paired Student's t-tests were used for identifying significant differences in the position of FMs with and without pelvic REs. Pearson's correlation analysis was used to explore the relationship between the direction of the pelvic REs and the difference in the position of FMs. A Wilcoxon signed-rank test was used to determine significant differences in DVH parameters between scenarios A and B, and between the original planned dose and cumulative delivered dose in scenarios A and B. Spearman's rank correlation coefficients were used to explore the relationship between the direction of pelvic REs and the differences in DVH parameters. A P-value of < 0.05 was considered significant for all statistical tests.

Results

Pelvic REs and displacement of FMs

Table 1 shows the pelvic REs and the displacement of FMs before and after correction of the pelvic REs during the treatment for 10 patients.

The means of pelvic REs \pm standard deviations (SD) were -0.2 ± 0.6 , 0.2 ± 0.7 , 0.3 ± 1.2 for yaw, roll, and pitch, respectively. The SD of the pitch direction was larger than that of the yaw and roll directions.

The displacement of the FMs were significantly different in the vertical and lateral directions ($p < 0.001$). In the vertical direction, the displacements of the FMs exceeding the PTV margin of PLNs were reduced by correcting the pelvic REs, as shown in Supplementary File — Figure S2. In the lateral direction, these were not observed at distances of more than 5 mm with or without pelvic REs.

In the vertical and lateral directions, difference in the position of the FMs before and after the correction of pelvic REs were strongly correlated with the pelvic REs of the pitch and yaw directions, respectively, as shown in Supplementary File — Figure S3. In the longitudinal direction, the displacement of the FMs had no significant correlation with the

Table 1. Displacement of fiducial markers (FMs) before and after the correction of the pelvic rotational errors (REs) during treatment course for 10 patients

Patient no	Before correction of pelvic REs						After correction of pelvic REs		
	Displacement of FMs [mm]			Pelvic REs [deg]			Displacement of FMs [mm]		
	Ver	Long	Lat	Yaw	Roll	Pitch	Ver	Long	Lat
1	-1.1 (1.0)	0.6 (1.1)	-0.1 (0.3)	-0.4 (0.2)	-0.2 (0.4)	0.5 (0.6)	-1.3 (1.1)	0.4 (1.0)	0.1 (0.4)
2	-0.9 (1.5)	-2.3 (1.5)	0.0 (0.5)	-0.6 (0.4)	-0.6 (0.5)	1.8 (0.6)	-3.0 (1.8)	-2.4 (1.2)	0.3 (0.4)
3	6.2 (1.7)	5.5 (1.7)	0.8 (0.4)	0.4 (0.5)	0.5 (0.5)	-0.6 (1.1)	6.2 (1.5)	5.4 (1.8)	0.2 (0.4)
4	6.2 (2.0)	2.9 (1.9)	0.7 (0.4)	0.1 (0.3)	0.2 (0.3)	0.7 (0.3)	4.4 (2.0)	2.3 (1.9)	0.7 (0.3)
5	3.4 (1.5)	2.8 (3.2)	-0.4 (0.5)	-0.8 (0.3)	-0.2 (0.3)	0.7 (0.4)	2.2 (1.6)	2.4 (2.8)	0.3 (0.4)
6	2.0 (1.7)	-0.3 (1.5)	0.8 (0.4)	0.3 (0.4)	0.5 (0.5)	0.8 (0.7)	1.1 (1.5)	-0.7 (1.2)	0.8 (0.3)
7	-1.2 (1.3)	-0.4 (1.5)	-0.1 (0.7)	-0.9 (0.7)	0.1 (0.7)	-1.9 (0.9)	0.4 (1.0)	-0.5 (1.5)	0.6 (0.4)
8	2.9 (1.2)	2.8 (1.3)	0.6 (0.6)	-0.2 (0.5)	0.7 (0.4)	0.0 (1.0)	2.6 (1.3)	2.8 (1.4)	0.2 (0.3)
9	1.0 (1.5)	-0.2 (2.2)	-0.3 (0.5)	-0.8 (0.4)	-0.1 (0.6)	1.0 (0.4)	0.3 (1.2)	0.5 (2.0)	0.3 (0.4)
10	-3.2 (1.6)	-2.6 (0.9)	0.1 (0.4)	0.1 (0.5)	1.3 (0.7)	0.2 (0.7)	-3.3 (1.2)	-2.4 (0.9)	0.0 (0.3)
Mean (SD)	1.5 (3.4)	0.9 (3.0)	0.2 (0.6)	-0.2 (0.6)	0.2 (0.7)	0.3 (1.2)	0.9 (3.2)	0.8 (2.9)	0.4 (0.4)
p							< 0.001	0.245	< 0.001

Ver — vertical; Long — longitudinal; Lat — lateral; SD — standard deviations; values in parentheses are standard deviation

pelvic REs. Correlations between the directions of the pelvic REs and the 3D displacements of the FMs are shown in Supplementary File — Table S1.

Differences in DVH parameters from planned dose for each scenario

For all fraction doses, the mean percentage differences ± standard error for CTV_{LN} (Gy) were -0.8 ± 0.1% in scenario A and -0.6 ± 0.1% in scenario B. Although there was a significant difference in the CTV_{LN} between scenario A and B (p = 0.022), the mean decrease rate was less than 1%. The D_{2cc} of the small bowel increased more in scenario A than in scenario B (2.4 ± 0.3% and 0.2 ± 0.3%, respectively; p < 0.001). The differences in V_{45Gy} of the small bowel in scenario A were larger than those in scenario B (1.9 ± 0.2% and 1.0 ± 0.1%, respectively; p < 0.001).

Correlations between the pelvic REs and difference in DVH parameters

Figure 2 shows the relationship between the pelvic REs in the pitch direction and the difference in DVH parameters between scenario A and B. The DVH parameters of the small bowel were strongly correlated with the pitch direction. Correlations between the direction of pelvic REs and the difference in DVH parameters between scenarios A and B are shown in Supplementary Table 2.

Comparison of the planned dose with the cumulative delivered dose in scenarios A and B

Table 2 shows the DVH parameters of the original planned and cumulative delivered doses in scenarios A and B for 10 patients. The mean delivered doses for ten patients were within -0.2% of the planned dose in both scenarios, with not significant difference. For the D_{2cc} and V_{45Gy} of the small bowel, the delivered doses were higher in scenario A, the maximum difference was observed in patient No. 4. However, the DVH parameters of the small bowel showed no significant difference between the two scenarios and planned doses.

Discussion

We examined the changes in the 3D position of FMs due to the pelvic REs and estimated on the PLNs coverage and the dose to the small bowel. Although the positions of FMs were significantly different in the vertical direction after the correction of pelvic REs, the dosimetric effect of pelvic REs on the dose to PLNs and the small bowel was negligible.

For the prostate-only radiotherapy, IC is placed close to the centroid of the implanted FMs [13]. When VISICOIL™ is used for IGRT, the ExacTrac software can detect the endpoint of two VISI-

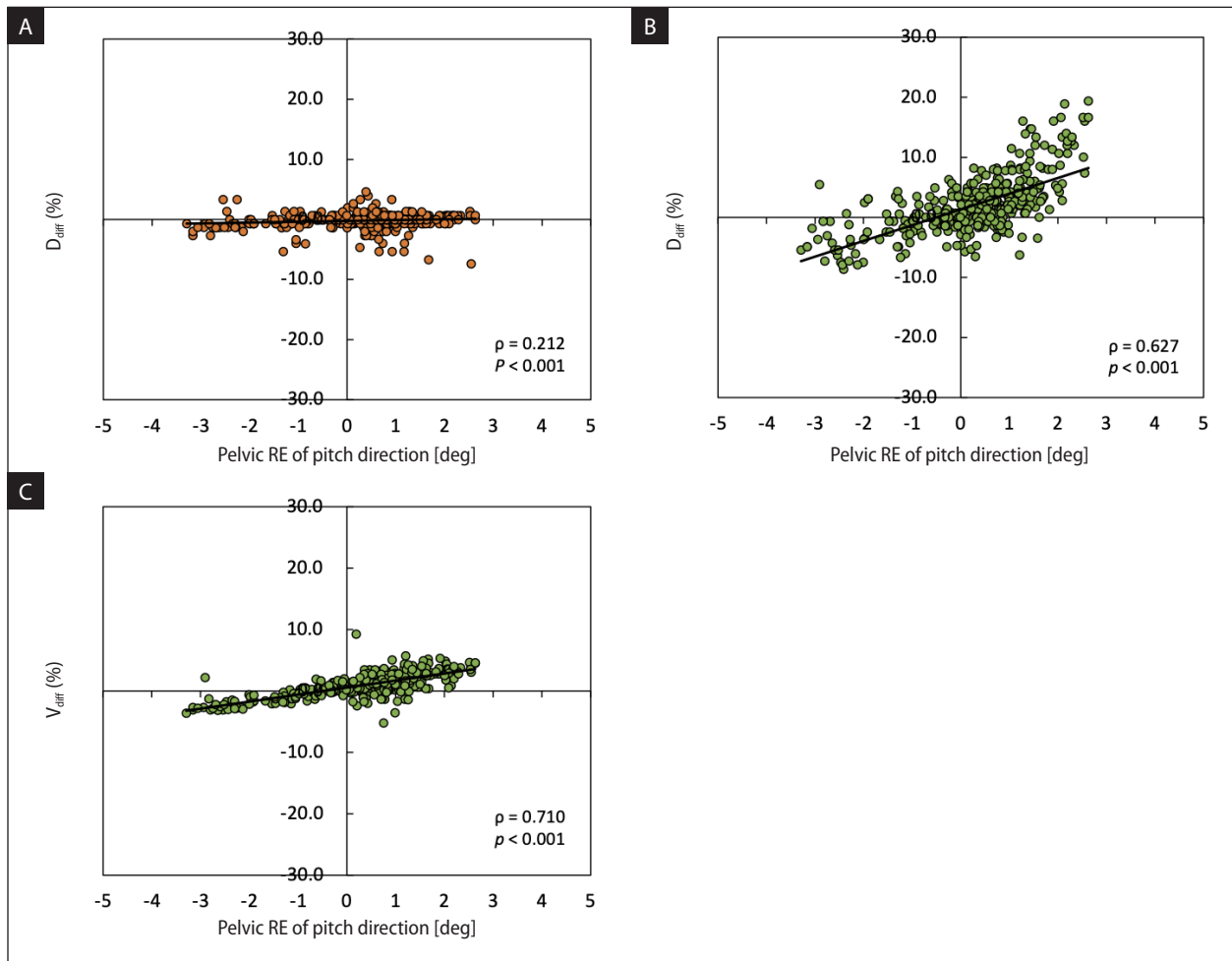


Figure 2. Relationship between pelvic rotational errors (REs) in the pitch direction and the differences in the following dose volume histogram (DVH) parameters: **(A)** $D_{98\%}$ of clinical target volume — CTV (CTV_{LN}), **(B)** D_{2cc} , and **(C)** V_{45Gy} of the small bowel between scenarios A and B for each fraction. The horizontal axis indicates the pelvic REs of the pitch direction

COILs (total four points), and then the position of FMs can be determined by “6 D calculation”. Tanabe et al. [14] reported that the magnitude of IC shifts between FM-based IGRT using ExacTrac and CBCT-based was highly correlated. In contrast, when the IC position does not correspond to the prostate, the position of FMs must be determined by “3D calculation” after manually aligning the FMs between the radiographs and DRRs. This is because, if the position of FMs is determined by 6D calculation considering the rotation of the prostate itself, the position of the entire pelvis would be significantly moved from the planned position.

The 3D displacement of FMs caused by the pelvic REs is associated with the distance between the FMs and the IC position [15]. The SD of the pelvic REs in the pitch direction was greater than that in the yaw and roll directions, consistent with previ-

ous reports [9, 18]. Thus, the position of FMs was strongly affected by the movement of field edge resulting from the pitch rotation of the pelvis in addition to the bladder volume and rectal filling, and large displacements of the FMs occurred in the vertical direction. Conversely, displacements of the FMs in the lateral direction were less than 5 mm, despite the addition of the pelvic rotation in the yaw direction.

With or without the pelvic REs, the position of the prostate is corrected based on the position of the FMs. In contrast, the PLNs and small bowel in the opposite direction might be affected by the change in the magnitude of IC shifts resulting from the pelvic REs. We simulated the IC shifts to evaluate the dose to the PLNs and the small bowel with and without pelvic REs. For each fraction dose, the $D_{98\%}$ of CTV_{LN} in scenario A was slightly lower than

Table 2. Dose volume histogram (DVH) parameters of the original plan and cumulative delivered dose of scenarios A and B in 10 patients

Patient no	CTV _{LN}			Small bowel					
	D _{98%} [Gy]			D _{2cc} [Gy]			V _{45Gy} (%)		
	Plan	A	B	Plan	A	B	Plan	A	B
1	58.4	58.4	58.4	47.7	48.6	45.1	0.8	0.9	0.6
2	58.7	58.9	58.8	58.5	60.3	54.4	4.9	5.4	2.8
3	58.7	57.9	57.9	67.6	64.0	66.9	12.0	14.3	16.0
4	59.0	58.3	59.0	55.3	60.7	58.8	8.5	15.3	12.8
5	59.0	59.4	59.4	59.6	60.9	60.5	15.3	20.6	18.8
6	58.8	59.0	59.0	55.8	58.0	57.3	11.7	14.2	13.4
7	58.7	58.7	58.9	64.1	61.2	64.9	9.4	7.9	9.9
8	58.6	58.8	58.8	56.3	58.6	58.3	17.3	19.5	19.3
9	58.9	59.3	59.1	58.2	58.5	58.3	11.0	12.0	11.7
10	58.8	58.3	57.5	55.4	53.0	51.3	8.2	5.7	4.5
Mean	58.8	58.7	58.7	57.9	58.4	57.6	9.9	11.6	11.0
SD	0.2	0.5	0.5	5.1	4.2	6.0	4.5	6.1	6.2
p		0.734	0.625		0.770	0.922		0.131	0.232

CTV — clinical target volume; SD — standard deviation

that in scenario B. In the vertical direction, IC shifts exceeding the PTV margin of PLN occurred frequently in scenario A because the displacements of the prostate caused by the pelvic REs added motion to the prostate itself. The change in DVH parameters of the small bowel was associated with the magnitude of the IC shift and pitch rotation because of the close proximity to high-dose regions (PTV_{LN}). When pitch rotation of the pelvis occurred in the positive direction, the region of the small bowel in the superior field edge was shifted to the side of the PTV_{LN}. At the same time, the position of FMs was displaced in the anterior direction. Thus, after performing prostate matching, the small bowel region was strongly shifted towards the PTV_{LN}.

Pelvic REs are always present during setup for any course of treatment [9, 18]. We estimated the delivered dose to the PLNs and small bowel taking both of daily IC shifts and pelvic REs into account during the treatment course. The DVH parameters of PLNs and small bowel were not significantly different between the planned dose and cumulative delivered dose. This is because any event producing atypical prostate displacement and pelvic REs during the treatment course will affect few fractions and will not have a significant effect on the cumulated dose distribution [10]. Moreover, if the pelvic REs in each direction would occur with equal

probability during the treatment course, the effects of positive and negative shifts would tend to cancel out [8].

To the best of our knowledge, this is the first study to estimate the dose to PLNs and small bowel under condition that the daily pelvic REs is considered. In previous studies, the dose to PLNs and small bowel was estimated only by 3D shift. Data on daily pelvic REs are limited, and that makes our study novel. 6D correction of pelvic REs requires orthogonal kV or CBCT images in addition to the images obtained by performing the FMs matching. In particular, CBCT imaging is associated with a long image acquisition time and a high radiation dose to the patient. Our results indicated that the pelvic REs should be corrected only when the systematic errors occur in the pitch direction. In clinical practice, translational errors can easily be corrected online using couch shifts along three axes. However, the correction of pelvic REs requires the 6D robotic couch. Accordingly, when correcting REs is difficult, attention should be paid to systematic REs in the pitch direction.

Our study has some limitations. First, we applied the same margin to the CTV_{LN} for both scenarios because this study was designed to focus on the change in DVH parameters by the pelvic REs. When the pelvic REs cannot be corrected, a higher

margin may be needed between the CTV and PTV [17]. Kershaw et al. [18] reported that the margin for the PLNs during bone matching can be smaller for the 6D couch than for the 3D couch in the vertical direction. Their results were similar to our results, i.e., the correction of REs in the pitch direction can be eliminated by the displacement of PLNs in the vertical direction. Second, for one patient, IGRT was performed using only one VISICOIL because the marker migration occurred before the treatment. However, we investigated the difference in the 3D position of FMs before and after pelvic REs. Thus, we believe that the impact of the number of the FMs on our results is small. Third, we focused on the dose to small bowel as the OAR in the opposite direction to the prostate. Although the dose to the rectum and bladder may be reduced by FM matching, those organs can exhibit daily variations in volume. Therefore, we will focus on the change in the dose using daily CBCT images.

Fourth, an interval between radiography assessments occurred between the first and second steps in the correction of pelvic REs. Thus, the difference in the position of FMs may have been affected slightly by the motion of the prostate itself [21, 22]. Fifth, all simulations during the treatment course were based on planning CT images. Therefore, the daily movement and deformation of the small bowel were not considered in the simulation [21]. The accuracy of the dose estimation on the PLNs and small bowel by using the daily CBCT images can be higher than the planning CT images. However, the regions of the PLNs and small bowel may leave out of the imaging region because the longitudinal field-of-view of CBCT was limited. Moreover, the CBCT images may have the imaging artifacts and may be the cause of decreased dose calculation accuracy.

Conclusion

We examined the impact of pelvic REs on the position of FMs and evaluated the effect of the correction of pelvic REs on the dose to PLNs and small bowels using the planning CT images. The position of FMs was strongly affected by the pitch rotation of the whole pelvis. If the systematic errors occur in the pitch direction, the dose of the small bowel region may be affected by the pelvic REs. However, the dosimetric effect of pelvic REs on the dose to

PLNs and the small bowel was negligible during the treatment course.

Conflict of interest

The authors have no conflicts of interest to declare that are relevant to the content of this article.

Funding

This work was supported by JSPS KAKENHI (Grant Number JP17K10481).

Acknowledgment

This work was supported by JSPS KAKENHI (Grant Number JP17K10481).

Ethics approval

This study was approved by our institutional ethics board (30-046).

Authors' contributions

Concept and design: H.K., S.T., T.S.; data analysis: H.K., T.K., A.O.; writing, reviewing and editing: H.K., S.T., T.K., A.O., T.S. All authors read and approved the final manuscript.

References

1. Gray PJ, Lin CC, Cooperberg MR, et al. Androgen deprivation with or without radiation therapy for clinically node-positive prostate cancer. *J Natl Cancer Inst.* 2015; 107(7): 729–737, doi: [10.1093/jnci/djv119](https://doi.org/10.1093/jnci/djv119), indexed in Pubmed: [25957435](https://pubmed.ncbi.nlm.nih.gov/25957435/).
2. van Nunen A, van der Toorn PPG, Budiharto TCG, et al. Optimal image guided radiation therapy strategy for organs at risk sparing in radiotherapy of the prostate including pelvic lymph nodes. *Radiother Oncol.* 2018; 127(1): 68–73, doi: [10.1016/j.radonc.2018.02.009](https://doi.org/10.1016/j.radonc.2018.02.009), indexed in Pubmed: [29501209](https://pubmed.ncbi.nlm.nih.gov/29501209/).
3. Chung HT, Xia P, Chan LW, et al. Does image-guided radiotherapy improve toxicity profile in whole pelvic-treated high-risk prostate cancer? Comparison between IG-IMRT and IMRT. *Int J Radiat Oncol Biol Phys.* 2009; 73(1): 53–60, doi: [10.1016/j.ijrobp.2008.03.015](https://doi.org/10.1016/j.ijrobp.2008.03.015), indexed in Pubmed: [18501530](https://pubmed.ncbi.nlm.nih.gov/18501530/).
4. Ghadjar P, Fiorino C, Munck Af Rosenschöld P, et al. ESTRO ACROP consensus guideline on the use of image guided radiation therapy for localized prostate cancer. *Radiother Oncol.* 2019; 141: 5–13, doi: [10.1016/j.radonc.2019.08.027](https://doi.org/10.1016/j.radonc.2019.08.027), indexed in Pubmed: [31668515](https://pubmed.ncbi.nlm.nih.gov/31668515/).
5. Eminowicz G, Dean C, Shoffren O, et al. Intensity-modulated radiotherapy (IMRT) to prostate and pelvic nodes-is pelvic lymph node coverage adequate with fiducial-based image-guided radiotherapy? *Br J Radiol.* 2014; 87(1037): 20130696, doi: [10.1259/bjr.20130696](https://doi.org/10.1259/bjr.20130696), indexed in Pubmed: [24646126](https://pubmed.ncbi.nlm.nih.gov/24646126/).

6. Adamczyk M, Piotrowski T, Adamiak E, et al. Dosimetric consequences of prostate-based couch shifts on the precision of dose delivery during simultaneous IMRT irradiation of the prostate, seminal vesicles and pelvic lymph nodes. *Phys Med.* 2014; 30(2): 228–233, doi: [10.1016/j.ejmp.2013.06.003](https://doi.org/10.1016/j.ejmp.2013.06.003), indexed in Pubmed: [23860339](https://pubmed.ncbi.nlm.nih.gov/23860339/).
7. Hsu A, Pawlicki T, Luxton G, et al. A study of image-guided intensity-modulated radiotherapy with fiducials for localized prostate cancer including pelvic lymph nodes. *Int J Radiat Oncol Biol Phys.* 2007; 68(3): 898–902, doi: [10.1016/j.ijrobp.2007.02.030](https://doi.org/10.1016/j.ijrobp.2007.02.030), indexed in Pubmed: [17459610](https://pubmed.ncbi.nlm.nih.gov/17459610/).
8. Kishan AU, Lamb JM, Jani SS, et al. Pelvic nodal dosing with registration to the prostate: implications for high-risk prostate cancer patients receiving stereotactic body radiation therapy. *Int J Radiat Oncol Biol Phys.* 2015; 91(4): 832–839, doi: [10.1016/j.ijrobp.2014.11.035](https://doi.org/10.1016/j.ijrobp.2014.11.035), indexed in Pubmed: [25752398](https://pubmed.ncbi.nlm.nih.gov/25752398/).
9. Guckenberger M, Meyer J, Vordermark D, et al. Magnitude and clinical relevance of translational and rotational patient setup errors: a cone-beam CT study. *Int J Radiat Oncol Biol Phys.* 2006; 65(3): 934–942, doi: [10.1016/j.ijrobp.2006.02.019](https://doi.org/10.1016/j.ijrobp.2006.02.019), indexed in Pubmed: [16751076](https://pubmed.ncbi.nlm.nih.gov/16751076/).
10. Rossi PJ, Schreiber E, Jani AB, et al. Boost first, eliminate systematic error, and individualize CTV to PTV margin when treating lymph nodes in high-risk prostate cancer. *Radiother Oncol.* 2009; 90(3): 353–358, doi: [10.1016/j.radonc.2008.09.021](https://doi.org/10.1016/j.radonc.2008.09.021), indexed in Pubmed: [18952307](https://pubmed.ncbi.nlm.nih.gov/18952307/).
11. Lawton CAF, Michalski J, El-Naqa I, et al. RTOG GU Radiation oncology specialists reach consensus on pelvic lymph node volumes for high-risk prostate cancer. *Int J Radiat Oncol Biol Phys.* 2009; 74(2): 383–387, doi: [10.1016/j.ijrobp.2008.08.002](https://doi.org/10.1016/j.ijrobp.2008.08.002), indexed in Pubmed: [18947938](https://pubmed.ncbi.nlm.nih.gov/18947938/).
12. Ferjani S, Huang G, Shang Q, et al. Alignment focus of daily image guidance for concurrent treatment of prostate and pelvic lymph nodes. *Int J Radiat Oncol Biol Phys.* 2013; 87(2): 383–389, doi: [10.1016/j.ijrobp.2013.06.003](https://doi.org/10.1016/j.ijrobp.2013.06.003), indexed in Pubmed: [23906929](https://pubmed.ncbi.nlm.nih.gov/23906929/).
13. Shang Q, Sheplan Olsen LJ, Stephans K, et al. Prostate rotation detected from implanted markers can affect dose coverage and cannot be simply dismissed. *J Appl Clin Med Phys.* 2013; 14(3): 4262, doi: [10.1120/jacmp.v14i3.4262](https://doi.org/10.1120/jacmp.v14i3.4262), indexed in Pubmed: [23652257](https://pubmed.ncbi.nlm.nih.gov/23652257/).
14. Tanabe S, Utsunomiya S, Abe E, et al. The impact of the three degrees-of-freedom fiducial marker-based setup compared to soft tissue-based setup in hypofractionated intensity-modulated radiotherapy for prostate cancer. *J Appl Clin Med Phys.* 2019; 20(6): 53–59, doi: [10.1002/acm2.12603](https://doi.org/10.1002/acm2.12603), indexed in Pubmed: [31054217](https://pubmed.ncbi.nlm.nih.gov/31054217/).
15. Liu H, Andrews M, Markovich A, et al. Dosimetric effect of uncorrected rotations in lung SBRT with stereotactic imaging guidance. *Phys Med.* 2017; 42: 197–202, doi: [10.1016/j.ejmp.2017.09.135](https://doi.org/10.1016/j.ejmp.2017.09.135), indexed in Pubmed: [29173916](https://pubmed.ncbi.nlm.nih.gov/29173916/).
16. Kaiser A, Schultheiss TE, Wong JYC, et al. Pitch, roll, and yaw variations in patient positioning. *Int J Radiat Oncol Biol Phys.* 2006; 66(3): 949–955, doi: [10.1016/j.ijrobp.2006.05.055](https://doi.org/10.1016/j.ijrobp.2006.05.055), indexed in Pubmed: [16949765](https://pubmed.ncbi.nlm.nih.gov/16949765/).
17. Zhang Q, Xiong W, Chan MF, et al. Rotation effects on the target-volume margin determination. *Phys Med.* 2015; 31(1): 80–84, doi: [10.1016/j.ejmp.2014.10.076](https://doi.org/10.1016/j.ejmp.2014.10.076), indexed in Pubmed: [25455438](https://pubmed.ncbi.nlm.nih.gov/25455438/).
18. Kershaw L, van Zadelhoff L, Heemsbergen W, et al. Image Guided Radiation Therapy Strategies for Pelvic Lymph Node Irradiation in High-Risk Prostate Cancer: Motion and Margins. *Int J Radiat Oncol Biol Phys.* 2018; 100(1): 68–77, doi: [10.1016/j.ijrobp.2017.08.044](https://doi.org/10.1016/j.ijrobp.2017.08.044), indexed in Pubmed: [29051038](https://pubmed.ncbi.nlm.nih.gov/29051038/).
19. Cramer AK, Haile AG, Ognjenovic S, et al. Real-time prostate motion assessment: image-guidance and the temporal dependence of intra-fraction motion. *BMC Med Phys.* 2013; 13(1): 4, doi: [10.1186/1756-6649-13-4](https://doi.org/10.1186/1756-6649-13-4), indexed in Pubmed: [24059584](https://pubmed.ncbi.nlm.nih.gov/24059584/).
20. Langen KM, Willoughby TR, Meeks SL, et al. Observations on real-time prostate gland motion using electromagnetic tracking. *Int J Radiat Oncol Biol Phys.* 2008; 71(4): 1084–1090, doi: [10.1016/j.ijrobp.2007.11.054](https://doi.org/10.1016/j.ijrobp.2007.11.054), indexed in Pubmed: [18280057](https://pubmed.ncbi.nlm.nih.gov/18280057/).
21. Nutting CM, Convery DJ, Cosgrove VP, et al. Reduction of small and large bowel irradiation using an optimized intensity-modulated pelvic radiotherapy technique in patients with prostate cancer. *Int J Radiat Oncol Biol Phys.* 2000; 48(3): 649–656, doi: [10.1016/s0360-3016\(00\)00653-2](https://doi.org/10.1016/s0360-3016(00)00653-2), indexed in Pubmed: [11020560](https://pubmed.ncbi.nlm.nih.gov/11020560/).